Supramolecular Chemistry
Publication details, including instructions for authors and subscription information:
http://www.informaworld.com/smpp/title~content=t713649759

Lead Ion Selective Signal Amplification by a Supramolecular Podand Fluoroionophore/Surfactant Complex Sensor in Water

Takashi Hayashita[a]; Dai Qing[a]; Richard A. Bartsch[b]; Sadik Elshani[b]; Robert E. Hanes[b]; Norio Teramae[a]
[a] Department of Chemistry, Graduate School of Science, Tohoku University, Sendai, Japan [b] Department of Chemistry and Biochemistry, Texas Tech University, Lubbock, TX, USA

To cite this Article Hayashita, Takashi , Qing, Dai , Bartsch, Richard A. , Elshani, Sadik , Hanes, Robert E. and Teramae, Norio(2005) 'Lead Ion Selective Signal Amplification by a Supramolecular Podand Fluoroionophore/Surfactant Complex Sensor in Water', Supramolecular Chemistry, 17: 1, 141 — 146
To link to this Article: DOI: 10.1080/10610270412331328899
URL: http://dx.doi.org/10.1080/10610270412331328899

Supramolecular Chemistry, January–March 2005 Vol. 17 (1–2), pp. 141–146

Taylor & Francis
Taylor & Francis Group

Lead Ion Selective Signal Amplification by a Supramolecular Podand Fluoroionophore/Surfactant Complex Sensor in Water

TAKASHI HAYASHITA[a,*], DAI QING[a], RICHARD A. BARTSCH[b], SADIK ELSHANI[b], ROBERT E. HANES JR[b] and NORIO TERAMAE*[a]

[a]*Department of Chemistry, Graduate School of Science, Tohoku University, Sendai 980-8578, Japan;* [b]*Department of Chemistry and Biochemistry, Texas Tech University, Lubbock, TX 79409, USA*

Received (in Austin, USA) 15 July 2004; Accepted 23 August 2004

Below the critical micelle concentration (cmc) of Triton X-100, a PD-18C6/Triton X-100 complex was found to exhibit an amplified fluorescence response for Pb^{2+} in water. No such signal amplification was noted above the cmc. Dynamic light scattering and dark-field microscope analyses revealed that the PD-18C6/Triton X-100 complex formed micron-size aggregates (1.24 ± 0.39 μm) triggered by selective Pb^{2+} binding, resulting in the enhancement of fluorescence intensity with a distinct blue shift of the fluorescence emission at pH 5.70. This is a novel supramolecular function of a PD-18C6/Triton X-100 complex sensor for selective Pb^{2+} recognition in water.

Keywords: Signal amplification; Lead ion recognition; Podand fluoroionophore; Triton X-100; Pseudo-micelle formation

INTRODUCTION

The design of selective and sensitive fluorescent chemosensors for trace metal ions is an important objective for chemistry, biology, and environmental science [1]. In particular, real-time and *in-situ* detection of toxic heavy metals, such as Pb^{2+}, in aqueous samples is a current issue [2, 3]. Although many practical fluoroionophores have been developed for heavy metal ions [4–6], the number of Pb^{2+}-selective fluoroionophores is still limited [7, 8]. For selective Pb^{2+} recognition, we have recently proposed a design concept based on: 1) a hard binding site constructed from O-donor atoms to reduce interaction with other relatively soft heavy metal ions; and, 2) a podand structure possessing a flexible pseudo-crown ether cavity to stabilize chelate complexes with Pb^{2+}, while reducing the interaction with alkali metal cations [9, 10]. Based on this concept, we have synthesized the podand fluoroionophore **PD-18C6** with a pseudocrown ether structure as the Pb^{2+} recognition site and proton-ionizable *N*-dansylacetamide as the photo-signal transduction moiety. Examination of the response function of **PD-18C6** to heavy metal ions in 70% 1,4-dioxane-30% water (v/v) revealed that the proton dissociation of **PD-18C6** was efficiently promoted by Pb^{2+} binding, resulting in a selective emission response for Pb^{2+} over the pH region from 4.0 to 5.0 [11].

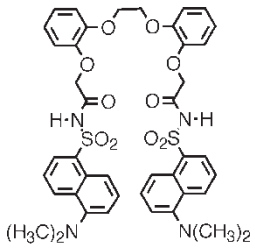

PD-18C6

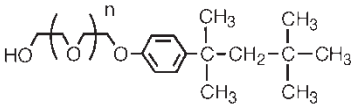

Triton X-100 (n = 9)

A micellar solution is expected to provide a hydrophobic microenvironment, which solubilizes lipophilic **PD-18C6** in water and enhances the metal/ionophore interaction [12–15]. It is interesting to probe how the microenvironment of the micelle affects the fluorescence response function of **PD-18C6** in water. In this study, we have found a unique

*Corresponding author. Fax: +81-22-217-6550. E-mail: haya@anal.chem.tohoku.ac.jp

ISSN 1061-0278 print/ISSN 1029-0478 online © 2005 Taylor & Francis Ltd
DOI: 10.1080/10610270412331328899

fluorescence signal amplification by a supramolecular **PD-18C6**/surfactant complex sensor for selective Pb^{2+} recognition in water. Below the critical micelle concentration (cmc) of the nonionic surfactant, Triton X-100, the **PD-18C6**/Triton X-100 complex forms pseudo-micelle aggregates triggered by selective Pb^{2+} binding, which results in enhancement of fluorescence intensity with a distinct blue shift of the fluorescence emission. We report herein this novel supramolecular function of the **PD-18C6**/Triton X-100 complex sensor for selective Pb^{2+} recognition in water.

RESULTS AND DISCUSSION

For micelle formation, we have chosen Triton X-100 as a nonionic surfactant, which has polyethylene glycol unit as a hydrophilic site and octylphenyl moiety as a hydrophobic site. The critical micelle concentration (cmc) of Triton X-100 is reported to be 0.24 mM in water [16]. In the presence of 10.0 mM Triton X-100 (above the cmc), **PD-18C6** (1.25×10^{-6} M) is readily dissolved in water. The pH-dependent changes in the fluorescence intensity of **PD-18C6** in the absence of metal ion (line 1) is compared with those in the presence of 5.0 mM Mg^{2+} (line 2) 5.0 mM Pb^{2+} (line 3) (Fig. 1a). In each system, the fluorescence intensities increase with increasing pH of the aqueous micellar solution. Similar to the 70% 1,4-dioxane-30% water (v/v) system [11], proton dissociation of **PD-18C6** is promoted by Pb^{2+} binding, and the Pb^{2+}-selective fluorescence emission is noted in the pH region from 4.0 to 5.0. Figure 1b shows the fluorescence spectra of **PD-18C6** at pH 4.29. Although the fluorescence change is moderate, an emission response is evident in the presence of 5.0 mM Pb^{2+}.

To elucidate the surfactant effect, the concentration of Triton X-100 was varied at pH 4.29. The resultant fluorescence intensity changes of **PD-18C6** as a function of the Triton X-100 concentration are depicted in Fig. 2a. In the presence of 5.0 mM Mg^{2+}, a typical sigmoid profile is obtained. Thus the fluorescence intensity increases markedly above the cmc (0.24 mM) of Triton X-100. Such a profile is known as a "micellar effect", in which

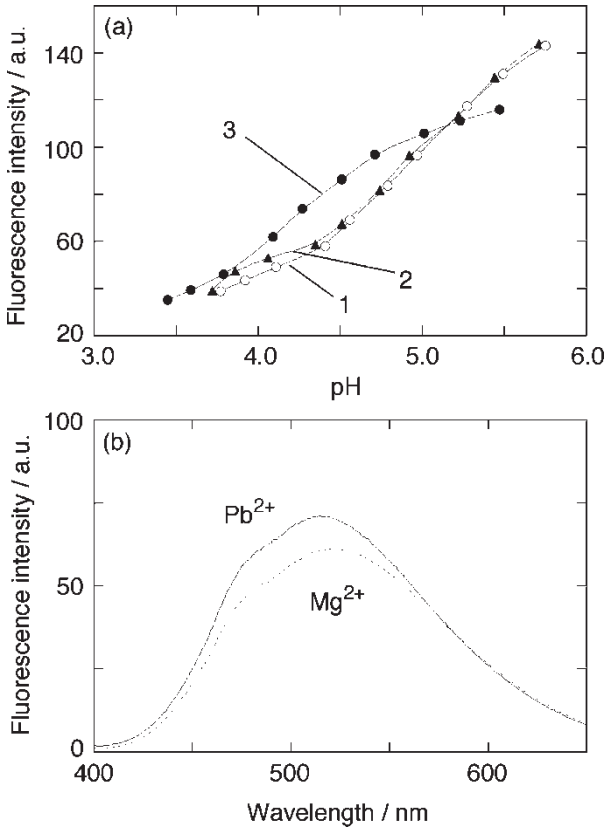

FIGURE 1 (a) Effect of pH upon fluorescence intensity of **PD-18C6** at 508.5 nm in the absence of metal ion (1), the presence of 5.0 mM Mg^{2+} (2), and 5.0 mM Pb^{2+} (3). (b) Fluorescence spectra of **PD-18C6** in the presence of 5.0 mM Mg^{2+} and Pb^{2+} at pH 4.29: [**PD-18C6**] = 1.25×10^{-6} M in 0.4% 1,4-dioxane-99.6% water (v/v) containing 10.0 mM Triton X-100 and 10.0 mM acetate buffer. The metal salts were $Mg(NO_3)_2$ and $Pb(NO_3)_2$. $\lambda_{ex} = 347.5$ nm.

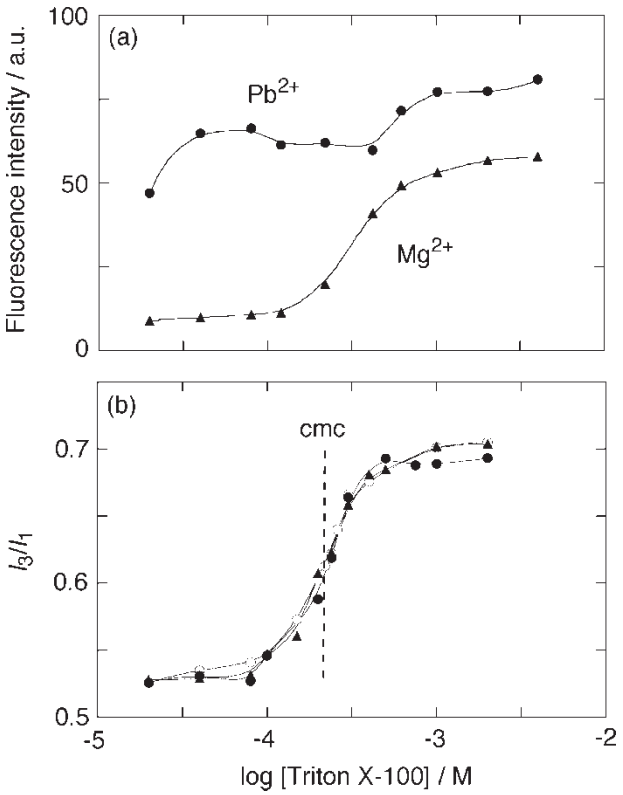

FIGURE 2 (a) Effect of Triton X-100 concentration upon fluorescence intensity of **PD-18C6** at 508.5 nm in the presence of 5.0 mM Mg^{2+} and 5.0 mM Pb^{2+}: [**PD-18C6**] = 1.25×10^{-6} M in 0.4% 1,4-dioxane-99.6% water (v/v) containing Triton X-100 and 10.0 mM acetate buffer (pH = 4.29). $\lambda_{ex} = 347.5$ nm. (b) Effect of Triton X-100 concentration upon the I_3/I_1 value of pyrene in the absence of metal ion (○), the presence of 5.0 mM Mg^{2+} (▲), and 5.0 mM Pb^{2+} (●): [pyrene] = 1.0×10^{-6} M in 0.5% 1,4-dioxane-99.5% water (v/v) containing Triton X-100 and 10.0 mM acetate buffer (pH = 4.29). The metal salts were $Mg(NO_3)_2$ and $Pb(NO_3)_2$. $\lambda_{ex} = 328$ nm.

the fluorescence quantum yield of the fluorophore is enhanced in the hydrophobic micellar phase due to reduction of the radiationless transition process for the fluorophore [17]. In the presence of 5.0 mM Pb^{2+}, however, quite a different pH-profile is noted. Interestingly, the fluorescence intensity remains high even below the cmc. As a result, efficient signal amplification for the Pb^{2+} response is found to be obtained below the cmc of Triton X-100 in water.

It is possible that Pb^{2+} interacts with the hydrophilic polyethylene glycol moiety of Triton X-100, which may interfere with the micelle formation process. To examine this possibility, a pyrene fluorophore with no Pb^{2+} recognition site was used as a polarity probe. The fluorescence intensity ratio (I_3/I_1) of pyrene is known to be sensitive for the microenvironment polarity around the pyrene, where the I_1 and I_3 represent the fluorescence intensities at the first peak (371.5 nm) and the third peak (382 nm), respectively. Thus the I_3/I_1 value can be used for evaluating micelle formation [17, 18]. As shown in Fig. 2b, the I_3/I_1 value clearly increases above the cmc. Similar to the blank (absence of metal ion), no influence upon micelle formation is noted in the presence of 5.0 mM Pb^{2+}. Thus the interaction of Pb^{2+} with Triton X-100 can be excluded for the micelle formation process.

The other possibility for signal amplification is an aggregate formation of **PD-18C6**/Triton X-100 complexes induced by Pb^{2+} binding with **PD-18C6**. In the absence of Triton X-100, an aqueous solution of **PD-18C6** shows turbidity due to the low solubility of **PD-18C6** in water. However even below the cmc, **PD-18C6** can be homogeneously dispersed in water in the presence of Triton X-100 by forming a **PD-18C6**/Triton X-100 complex. In the presence of Pb^{2+}, we assume that the micelle-like structure of **PD-18C6**/Triton X-100 complexes (pseudo-micelle aggregates) is induced by formation of a hydrophobic core due to Pb^{2+} binding with **PD-18C6** in water (Fig. 3). To probe this possibility, dynamic light scattering analysis was performed. The resultant histograms are shown in Fig. 4. For the Mg^{2+} system, **PD-18C6**/Triton X-100 complex is dissolved

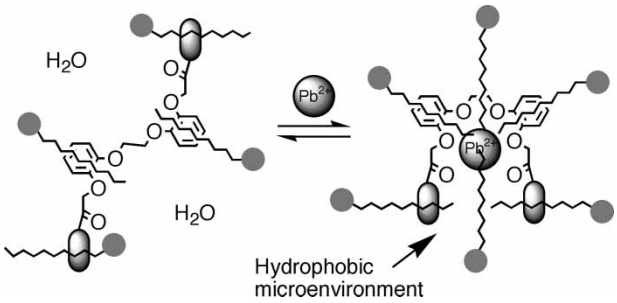

FIGURE 3 Fluorescence signal amplification mechanism based on pseudo-micelle aggregate formation.

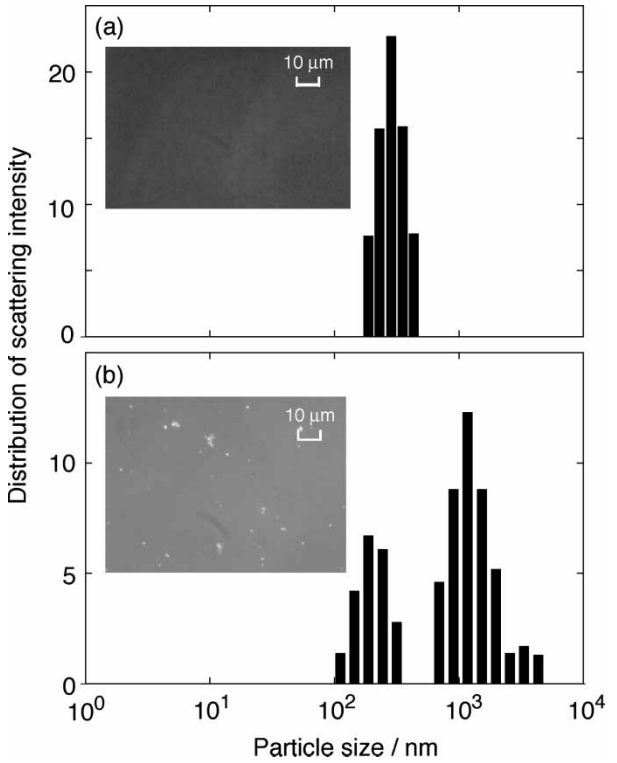

FIGURE 4 Distribution of light scattering intensity as a function of particle size in the presence of 5.0 mM Mg^{2+} (a) and 5.0 mM Pb^{2+} (b). The inset pictures represent the results for dark-field microscope analysis: [**PD-18C6**] = 3.0×10^{-6} M in 0.4% 1,4-dioxane-99.6% water (v/v) containing 0.08 mM Triton X-100 and 10.0 mM acetate buffer (pH 4.29). The metal salts were $Mg(NO_3)_2$ and $Pb(NO_3)_2$.

in water as nano-size aggregates of 293.7 ± 71.2 nm. Whereas in the presence of Pb^{2+}, micron-size aggregates (1236.8 ± 386.2 nm) are further generated in addition to the nano-size aggregates (206.8 ± 59.1 nm). The formation of micron-size aggregates in the presence of 5.0 mM Pb^{2+} is directly confirmed with a dark field microscope analysis (inset in Fig. 4b). These results strongly support the Pb^{2+} response mechanism presented in Fig. 3.

Figure 5a shows the pH-dependent fluorescence intensity changes of **PD-18C6** in the presence of 0.08 mM Triton X-100. Below the cmc, the aggregate formation of **PD-18C6**/Triton X-100 complex makes the pH-profiles complicated. For the Mg^{2+} system, the fluorescence intensity decreases with increasing pH from 3.4 to 4.3, then increases for pH values above 4.3. On the other hand, the fluorescence intensity increases monotonously with an increase in pH for the Pb^{2+} system. The factors of the fluorescence quenching by water [19], the fluorescence intensity changes by proton-dissociation of the dansylacetamide moiety [11, 20], and the pseudo-micellar effect [17] complicate these pH profiles. The open symbols are results from a duplicate experiment, indicating good reproducibility for the present system within experimental error.

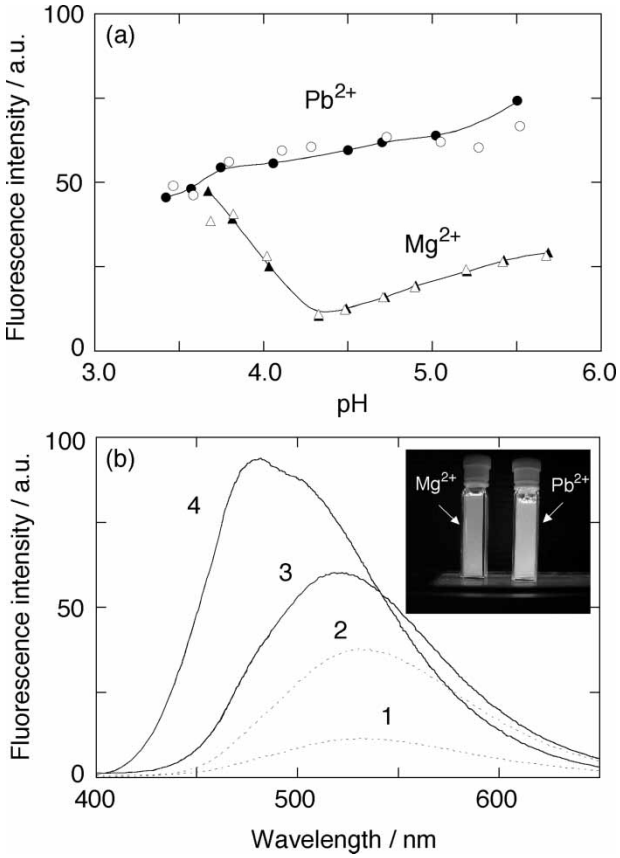

FIGURE 5 (a) Effect of pH upon fluorescence intensity of **PD-18C6** at 508.5 nm in the presence of 5.0 mM Mg^{2+} and 5.0 mM Pb^{2+}. Open symbols represent the results from a duplicate experiment. (b) Fluorescence spectra of **PD-18C6** in the presence of 5.0 mM Mg^{2+} (line 1: pH 4.29; line 2: pH 5.70) and 5.0 mM Pb^{2+} (line 3: pH 4.29; line 4: pH 5.70). The inset shows the fluorescences corresponding to spectra 2 and 4: [**PD-18C6**] = 1.25×10^{-6} M in 0.4% 1,4-dioxane-99.6% water (v/v) containing 0.08 mM Triton X-100 and 10.0 mM acetate buffer. The metal salts were $Mg(NO_3)_2$ and $Pb(NO_3)_2$. $\lambda_{ex} = 347.5$ nm.

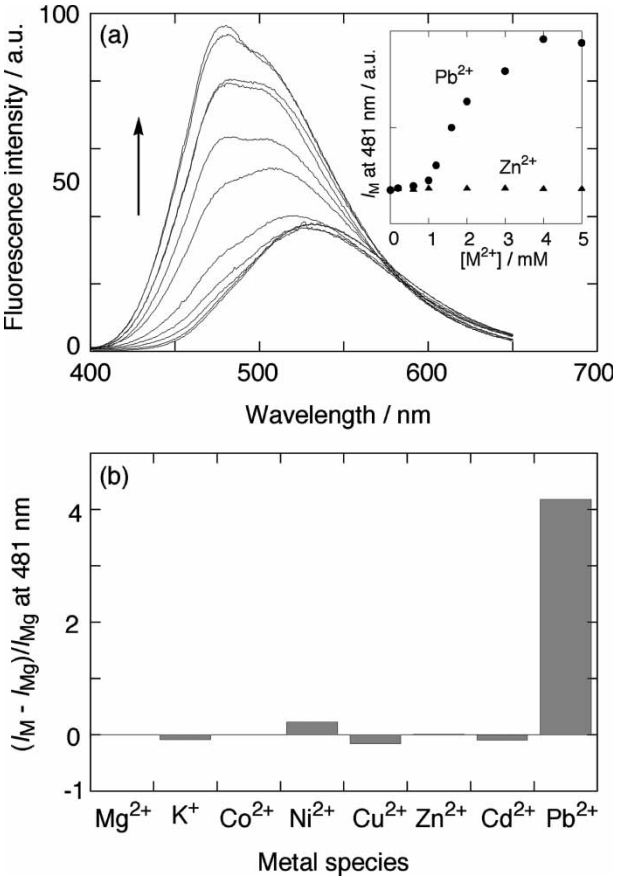

FIGURE 6 (a) Effect of Pb^{2+} concentration upon fluorescence spectra of **PD-18C6**. Inset figure shows the effect of pH upon the fluorescence intensity of **PD-18C6** at 481 nm: [**PD-18C6**] = 1.25×10^{-6} M in 0.4% 1,4-dioxane-99.6% water (v/v) containing 0.08 mM Triton X-100 and 10.0 mM acetate buffer (pH 5.70). (b) Fluorescence response selectivity for various metal ion species: [**PD-18C6**] = 1.25×10^{-6} M in 0.4% 1,4-dioxane-99.6% water (v/v) containing 0.08 mM Triton X-100 and 10.0 mM acetate buffer (pH 5.70). I_M and I_{Mg} are the fluorescence intensities at 481 nm in the presence of 5.0 mM metal nitrate and 5.0 mM $Mg(NO_3)_2$, respectively. $\lambda_{ex} = 347.5$ nm.

In Fig. 5b are shown the fluorescence spectra of **PD-18C6**/Triton X-100 complex at pH 4.29 (spectra 1 for Mg^{2+} and 3 for Pb^{2+}) and at pH 5.70 (spectra 2 for Mg^{2+} and 4 for Pb^{2+}), respectively. In contrast to the fluorescence spectra in Fig. 1b, signal amplification for the Pb^{2+}-selective fluorescence response is apparent. It should be noted that a distinct blue shift of the fluorescence spectra is observed by addition of 5.0 mM Pb^{2+} at pH 5.70. Thus the fluorescence color changes from green ($\lambda_{max} = 531$ nm) to blue ($\lambda_{max} = 481$ nm), which is easily confirmed by the naked eye (inset in Fig. 5b).

The effect of Pb^{2+} concentration upon the fluorescence spectra of the **PD-18C6**/Triton X-100 complex at pH 5.70 is depicted in Fig. 6a. In the inset are shown the fluorescence intensity changes at 481 nm as a function of the metal ion concentration. Although the fluorescence intensity increases with an increase of Pb^{2+} concentration, an inductive region for the Pb^{2+} response is noted below 1.0 mM Pb^{2+}. This sigmoidal response may be based on the pseudo-micelle aggregate formation induced by Pb^{2+} binding, which causes a homotoropic allostery for the Pb^{2+} response [21]. Similar to Mg^{2+} system, no fluorescence response is noted upon addition of Zn^{2+}. The response selectivity for other metal ion species were examined by the relative fluorescence intensity changes of the metal ions to that of Mg^{2+} (Fig. 6b). It is evident that the **PD-18C6**/Triton X-100 complex exhibits a high response selectivity for Pb^{2+} over other metal ions, such as Mg^{2+}, K^+, Co^{2+}, Ni^{2+}, Cu^{2+}, Zn^{2+}, and Cd^{2+}, with a unique fluorescence signal amplification in water.

In conclusion, the **PD-18C6**/Triton X-100 complex formed below the cmc in water is found to exhibit an amplified fluorescence response for Pb^{2+}. Dynamic light scattering and dark-field microscope analyses reveal that the **PD-18C6**/Triton X-100 complex forms pseudo-micelle aggregates, triggered by selective Pb^{2+} binding with **PD-18C6**, which results in

enhancement of fluorescence intensity with a distinct blue shift of the fluorescence emission at pH 5.70. Although the present system exhibits a low sensitivity due to the presence of an inductive region for the Pb^{2+} response, the sensitivity could be improved by a proper combination of the podand binding site and a surfactant species with a low cmc or by incorporating the amphiphilic function in the podand fluoroionophore to induce self-aggregation in water. These approaches are actively in progress in our laboratories.

EXPERIMENTAL

Apparatus

Fluorescence spectra were measured by a JASCO FP-777W spectrophotometer (Japan Spectroscopic Co. Ltd.) at 25 °C; the slits for the excitation and emission monochrometers were 3.0 nm and 1.5 nm, respectively; and the spectral scan rate was 50.0 nm/min. All fluorescence spectra were excited at 347.5 nm, which is the isosbestic point of the UV-Vis spectrum of **PD-18C6** in a 70% 1,4-dioxane-30% water (v/v) system. Absorption spectra were recorded with a Hitachi U-3000 UV-Vis spectrophotometer (Hitachi, Ltd.) with a quartz cell of 5.0-cm path length at 25 °C. ^{1}H-NMR spectra were taken with a Varian Gemini 300 nuclear magnetic resonance spectrometer. IR spectra were measured with Perkin-Elmer Model 1600, Model 297, and Nicolet MS-X infrared spectrophotometers. The aggregate size was analyzed with a dynamic light scattering spectrophotometer (FPAR-1000, Otsuka Electronics Co., Ltd.). The dark field microscope analysis was performed with an Olympus Power BX51 instrument. Combustion analyses were performed by Desert Analytics Laboratory of Tucson, Arizona.

Reagents

Pyrene (analytical grade, Wako Pure Chemical Industries, Ltd.) was purified by sublimation. Polyoxyethylene (10) octylphenyl ether (Triton X-100) was purchased from ICN Biomedical Inc. 1,4-Dioxane (specially prepared reagent for HPLC) was obtained from Nacalai Tesque, Inc. All other solvents and reagents were obtained at the highest commercial quality and used without further purification. The pH of 0.10 M acetate buffer solutions were adjusted by tetramethylammonium hydroxide (TMAOH, 15 wt% aqueous solution, Wako Pure Chemical Industries, Ltd.), and these buffer solutions were used by diluting 1/10. All aqueous solutions were prepared with distilled water that was subsequently deionized using a Millipore Milli-Q water system.

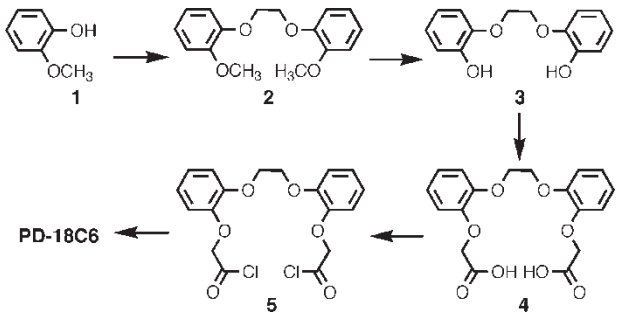

Preparation of 1,2-Bis(2′-methoxyphenoxy) ethane (2)

A solution of guiacol (**1**) (5.00 g, 4.03 mmol) in MeCN (100 mL) was purged with nitrogen for 30 min. The nitrogen flow was reduced and Cs_2CO_3 (14.92 g, 44.8 mmol) was added. With vigorous magnetic stirring, the mixture was refluxed for 3 h and then a solution of ethylene glycol ditosylate (6.95 g, 18.3 mmol) in MeCN (50 mL) was added dropwise. After stirring at reflux for another 24 h, the mixture was allowed to cool to room temperature and then filtered through a pad of Celite. The Celite pad was rinsed with CH_2Cl_2. The filtrate and rinsing were evaporated *in vacuo* and the residue was dissolved in CH_2Cl_2. The solution was washed sequentially with 50 mL each of 1 N aqueous NaOH, brine, and distilled water, dried over $MgSO_4$, and evaporated *in vacuo*. The residue was chromatographed on alumina with CH_2Cl_2 as eluent. The resultant white solid was recrystallized from EtOAc to give 4.97 g (90%) of **2** with mp 133–135 °C (mp 138–140 °C [22]): IR (deposit from $CDCl_3$ onto a NaCl plate): 1256, 1123, 1070 cm^{-1}; ^{1}H NMR ($CDCl_3$): δ 3.85 (s, 6H); 4.41 (s, 4H); 6.84–7.02 (m, 8H).

Preparation of Bisphenol 3

In a 3-necked flask equipped with a water condenser, 2,4,6-collidine (50 mL) was purged with nitrogen for 15 min using a gas dispersion tube below the surface of the solvent. The nitrogen flow was reduced and 9.76 g (35.6 mmol) of **2** and 9.77 g (73 mmol) of anhydrous LiI were added. Stirring was initiated and the temperature was increased (~10 °C/min) until it reached 150 °C. After stirring and heating at this temperature for 3 h, the mixture was allowed to cool to room temperature. The 2,4,6-collidine was removed by simple distillation under high vacuum. To the residue under nitrogen, 1 N HCl (250 mL) and CH_2Cl_2 (100 mL) were added. After stirring the mixture for 15 min, the organic layer was separated and the aqueous layer was extracted with CH_2Cl_2 (100 mL). The combined organic layer and extract were washed with 6 N HCl (2 × 100 mL), water (2 × 100 mL), and brine (100 mL), dried over $MgSO_4$,

and evaporated *in vacuo.* Bisphenol **3** (7.00 g, 80%) was isolated as a white solid with mp 112–114 °C (mp 115–116 °C [23]): IR (deposit from $CDCl_3$ solution onto a NaCl plate): 3410 (O—H); 1220, 1106 (C-O) cm^{-1}; ^1H NMR ($CDCl_3$): δ 4.39 (s, 4H); 5.71, (s, 2H); 6.83–6.95 (m, 8H).

Preparation of Polyether Dicarboxylic Acid 4

A mixture of NaH (1.20 g, 50 mmol) and THF (30 mL) was stirred under nitrogen for 30 min at room temperature and then a solution of bisphenol **3** (1.23 g, 5.0 mmol) in THF (50 mL) was added dropwise over a 1-h period. The mixture was stirred for 1 h at room temperature and then a solution of bromoacetic acid (2.78 g, 20 mmol) in THF (50 mL) was added over a 2 h period. The mixture was stirred for 5 h at room temperature, then refluxed overnight. Water was added carefully to destroy the excess NaH and the THF was evaporated *in vacuo*. Water was added to the residue and the mixture was acidified with 6 N HCl, forming a white solid. Attempted extraction of the aqueous mixture with CH_2Cl_2 left the solid between the aqueous and CH_2Cl_2 layers. The solid was filtered, washed with water, allowed to air-dry, and then refluxed with toluene. After cooling to room temperature, the solid was filtered and recrystallized from a small amount of MeOH. A white solid with mp 165–167 °C was obtained (11.58 g, 64%): IR (KBr): 3426 (OH), 1739 (C = O) cm^{-1}. ^1H NMR ($CDCl_3$): δ 4.45 (s, 4H), 4.66 (s, 4H), 6.89-7.05 (m, 8H), 7.48 (s, 2H). Anal. Calcd for $C_{18}H_{18}O_8$: C, 59.67; H, 5.07. Found: C, 59.52; H, 5.00.

Preparation of PD-18C6

To a solution of **4** (1.81, 5.0 mmol) in benzene (30 mL) at 0 °C under nitrogen, oxalyl chloride (6.35 g, 50 mmol) was added dropwise. The reaction mixture was stirred for 1 h at room temperature and then for 1 h at reflux. After evaporation of the benzene and excess oxalyl chloride *in vacuo*, diacid chloride **5** was used immediately in the next step. The acid chloride was dissolved in THF (30 mL) and added to a mixture of NaH (1.20 g, 50.0 mmol) and dansylamide (2.75, 11.0 mmol) in THF (40 mL) under nitrogen. The mixture was stirred at room temperature for 10 h and cooled to 0 °C. Water was added carefully to destroy the excess NaH and the THF was evaporated *in vacuo*. Water was added to the residue and the mixture was extracted with CH_2Cl_2. The organic layer was washed with water, dried over Na_2SO_4, and evaporated *in vacuo*. The residue was chromatographed on silica gel with CH_2Cl_2 then CH_2Cl_2-EtOAc (4:1) as eluents to give a solid that was dissolved in CH_2Cl_2 (150 mL) and washed with 1 N HCl (100 mL). The organic solution was washed with water, dried over $NaSO_4$, and evaporated *in vacuo*. The residue was recrystallized from MeOH to give a 65% yield of **PD-18C6** with mp 148–150 °C: IR (deposit from CH_2Cl_2solution onto a NaCl plate): 3236 (NH), 1726 (C = O), 1389, 1202 (SO_2) cm^{-1}; ^1H NMR ($CDCl_3$): δ 2.84 (s, 12H), 4.45 (s, 4H), 4.66 (s, 4H), 6.85–6.88 (m, 4H), 7.04–7.17 (m, 6H), 7.26–7.32 (m, 2H), 7.54 (t, 6H, $J = 7.5$ Hz), 8.08 (d, 2H, $J = 8.7$ Hz), 8.47–8.50 (m, 2H), 8.56 (d, 2H, $J = 8.5$ Hz), 10.31 (s, 2H). Anal. Calcd for $C_{42}H_{42}N_4O_{10}S_2$: C, 61.00; H, 5.12; N, 6.78. Found: C, 60.71; H, 5.21; N, 6.63.

Acknowledgements

The authors acknowledge Mr. Y. Kon, Dr. A. Yamaguchi (Tohoku University), and Dr. K. Bessho (Radiation Science Center, High Energy Accelerator Research Organization) for their helpful discussions and experimental supports. This research was partly supported by Toray Science and Technology Grant and Grants-in-Aid for Scientific Research (c) (No. 16550066) from the Ministry of Education, Culture, Sports, Science and Technology, Japan. Research conducted at Texas Tech University was supported by Grant D-0775 from The Welch Foundation to RAB.

References

[1] *Chemosensors of Ion and Molecule Recognition*; Desvergne, J. P., Czarnik, A. W., Eds.; Kluwer: Dordrecht, 1997.
[2] Fetch, A. *Crit. Rev. Anal. Chem.* **1998**, *28*, 267.
[3] Yu, X.; Yuan, H.; Górecki, T.; Pawliszyn, J. *Anal. Chem.* **1999**, *71*, 2998.
[4] de Silva, A. P.; Fox, D. B.; Huxley, A. J. M.; Moody, T. S. *Coord. Chem. Rev.* **2000**, *205*, 41.
[5] Adendota, V.; Fabbrizzi, L.; Licchelli, M.; Mangano, C.; Pallavicini, P.; Parodi, L.; Poggi, A. *Coord. Chem. Rev.* **2000**, *192*, 649.
[6] Yamauchi, A.; Hayashita, T. *Bunseki Kagaku* **2000**, *49*, 75.
[7] Métiver, R.; Leray, L.; Valeur, B. *Chem. Commun.* **2003**, 996.
[8] Hayashita, T.; Dai Qing; Minagawa, M.; Lee, J. C.; Ku, C. H.; Teramae, N. *Chem. Commun.* **2003**, 2160.
[9] Hayashita, T.; Sawano, H.; Higuchi, T.; Indo, M.; Hiratani, K.; Zhang, Z.-Y.; Bartsch, R. A. *Anal. Chem.* **1999**, *71*, 791.
[10] Hayashi, R.; Hayashita, T.; Yoshikawa, T.; Hiratani, K.; Bartsch, R. A.; Teramae, N. *Bunseki Kagaku* **2003**, *52*, 755.
[11] Minagawa, M.; Hayashita, T.; Dai Qing; Bartsch, R. A.; Teramae, N. *Bunseki Kagaku* **2002**, *51*, 681.
[12] Hayashita, T.; Teramae, N.; Kuboyama, T.; Nakamura, S.; Yamamoto, H.; Nakamura, H. *J. Incl. Phenom.* **1998**, *32*, 251.
[13] Sakamoto, H.; Tanaka, M.; Kimura, K. *Chem. Lett.* **2000**, *29*, 928.
[14] Bhattacharya, S.; Gulyani, A. *Chem. Commun.* **2003**, 1158.
[15] Nakahara, Y.; Kida, T.; Nakatsuji, Y.; Akashi, M. *Chem. Commun.* **2004**, 224.
[16] Lin, H.-Y.; Thomas, J. L. *Langmuir* **2003**, *19*, 1098.
[17] Moroi, Y. *Micelles –Theoretical and Applied Aspects*; Plenum Press: New York, 1992.
[18] Kalyanasundaram, K.; Thomas, J. K. *J. Am. Chem. Soc.* **1977**, *99*, 2039.
[19] Macanita, A. L.; Costa, F. P.; Costa, S. M. B.; Melo, E. C.; Santos, H. *J. Phys. Chem.* **1989**, *93*, 336.
[20] Tong, A.-J.; Song, Y.-S.; Li, L.-D.; Hayashita, T.; Teramae, N.; Park, C.; Bartsch, R. A. *Anal. Chim. Acta* **2000**, *420*, 57.
[21] Takeuchi, M.; Ikeda, M.; Sugasaki, A.; Shinkai, S. *Acc. Chem. Res.* **2001**, *34*, 865.
[22] Pedersen, C. J. French Patent 1,440,716, 1966; *Chem. Abstr.* **1967**, *66*, 4411.
[23] Vögtle, F.; Weber, E. *Angew. Chem., Int. Ed. Engl.* **1980**, *19*, 1030.